Folding within seconds

Thomas Kenkmann*
Institut für Mineralogie, Museum für Naturkunde, Humboldt-Universität Berlin, D-10115 Berlin, Germany

ABSTRACT

Hypervelocity impacts of cosmic projectiles larger than ~200 m diameter are capable of forming complex craters on Earth. At these craters, shock loading, shock damage, and excavation flow are followed by a gravity-driven collapse of the deep transient cavity. Such impact structures are characterized by a central uplift, a flat crater floor, and a terraced crater rim. Collapse-induced deformation features, like folds and brittle fault zones, have many similarities to tectonic structures. Typical deformation patterns of complex terrestrial impact craters of 5–15 km diameter are compiled and analyzed with respect to their kinematic development. Unlike their tectonic counterparts, deformation structures are always the result of non-plane-strain deformation and are formed in a single event that takes place in seconds to minutes. To understand the high-strain-rate processes, the microstructure of an impact-induced fold of the Crooked Creek impact crater (~7 km diameter), Missouri, United States, is investigated in detail. A period of 20–30 s at the most is determined for the collapse phase of this crater. The gross plastic deformation behavior of the fold is achieved by localized brittle deformation along millimeter- to centimeter-spaced fault zones, forming a network of veins. Shock damage has fractured ~40% of grain boundaries. The onset of collapse and associated deformation started in rocks with a reduced cohesion and is friction controlled.

Keywords: folding, impact craters, cratering, brittle deformation, friction.

INTRODUCTION

A crucial problem in structural geology is the determination of the time period a certain structure, e.g., a fold, needs to develop. For time-dependent, ductile deformation processes, the duration of a deformation event is often unknown, which means that strain-rate–dependent deformation mechanisms, in nature, are incompletely defined. A direct comparison with experimental investigations, therefore, often can be difficult or ambiguous. Brittle deformation processes are largely time independent, but the deformation structures (faults and folds) of the upper crust are the result of myriads of deformation increments, superimposed one upon the other. Thus, we do not know what structural assemblage, if any, is the result of a single slip event.

A unique opportunity to define the period of rock deformation and, thus, to study a single deformation event is provided by impact craters on Earth, which formed in otherwise undeformed rocks. About 160 terrestrial impact craters have been discovered so far (Grieve, 1991), but many more are expected to exist within Earth's upper crust. The formation of an impact crater can be divided into three major stages, which form a continuum: (1) contact and compression, (2) excavation, and (3) modification. During the first stage, the kinetic energy is transferred from the impacting body to the target rocks, leading to the propagation of a shock wave, which spreads out hemispherically and travels with hypersonic speed. During the second stage, a deep, parabolically shaped, transient cavity is actually formed by particle motions produced by the shock and rarefaction wave. At the final stage, the unstable, transient cavity collapses under gravity (Melosh, 1989). Depending on the degree of collapse, the final craters are classified into simple or complex morphologies. On Earth, simple craters are 2–4 km in diameter and are characterized by a bowl-shaped depression with an elevated crater rim. In contrast, complex craters exhibit terraced walls, a flat floor, and an uplifted central area. With hydrocodes, it is possible to simulate a complete impact on a gross scale (e.g., Melosh and Ivanov, 1999) and to determine the time period of each cratering stage. Whereas shock deformation takes place on extremely short time scales compared to other geologic processes (Melosh, 1989), transient cavity collapse can be compared to brittle tectonic deformation and landslides, with respect to strain rate.

Major differences between gravity-driven collapse of large impact craters and upper crustal tectonics occur in the slip behavior and the particle trajectory field. As a first approximation, in an impact individual particle paths have a radial symmetry, with respect to the impact center, which results in the conditions for plane-strain deformation not being fulfilled. Shear displacements occur as single-slip events, with displacements ranging from millimeters to several kilometers (Spray, 1997). If the impact formed in a tectonically stable province of the continental crust, a later reactivation of faults can be neglected. In contrast, endogenic faults in the upper crust are normally formed by discontinuous motion (stick slip) over millions of years. These multislip events often provoke large total displacements, but individual slip events never exceed a few meters. Phases of sticking and seismic silence lead to healing of cracks and sealing of the shear zones. Changes in the boundary conditions during the deformation period (e.g., the state of stress) may lead to the superposition of different strain patterns within a single structure. The differing deformation histories of tectonic faults and folds, on the one hand, and impact-induced faults and folds, on the other, may lead to major differences in the final geometry of these structures. For example, the displacement/length ratio of faults may evolve in a different manner. Comparative studies of impact-induced and tectonic deformation structures are rare (Spray, 1997; Bjørnerud, 1998).

Impact-induced deformation features provide important information to structural geology, in several respects: They enable the analysis of (1) single-slip deformation events, (2) structures formed in a known period of time, and (3) non-plane-strain deformation, e.g., the

*E-mail: thomas.kenkmann@rz.hu-berlin.de.

effects of oblique collision. This approach makes terrestrial impact craters large-scale laboratories for structural investigations.

The investigation of impact-induced deformation structures is also required to achieve a better understanding of the kinematic history, the deformation mechanisms, and the rheological properties of rocks during transient cavity modification. For a characterization of deformation mechanisms, microstructural investigations of the deformation features are of crucial importance. Such investigations are particularly required to understand the anomalous low strength properties of crater floor rocks (McKinnon, 1978) and to assess the role that acoustic fluidization plays in the inferred strength reduction of the target material (Melosh, 1979).

POSTSHOCK DEFORMATION PATTERN OF COMPLEX IMPACT CRATERS

Deformation structures in the floor of terrestrial impact craters are complex and different. Such differences can be attributed to variations in a number of boundary conditions, including impact energy and impact angle, target composition and stratification, and target rheology. In addition, different levels of erosion at specific craters exhume different deformation features. Nevertheless, a number of common deformation structures can be identified in impact craters, where the crater floor is exposed. Figure 1 is an idealized map, showing typical structural elements in the parautochthonous rocks of the floor of a 5–15-km-diameter complex crater. The compilation is based on my structural studies at several complex craters in Europe and the United States (e.g., Kenkmann et al., 2000; Kenkmann and von Dalwigk, 2000) and geologic maps and publications on these and other complex impact craters (e.g., Wilshire et al., 1972; Roddy, 1979; Laney and Van Schmus, 1978; Offield and Pohn, 1979; Shoemaker and Shoemaker, 1996; Kriens et al., 1999). Effects of oblique impacts, which are able to produce asymmetries in structure and failure pattern (Schultz and Anderson, 1996), are not considered in the compilation.

The structural elements of complex impact craters can be separated into first- and second-order elements. As shown in Figure 1, first-order structural elements include a crater-rim normal fault or crater-rim monocline (I) defining the crater diameter. A monocline is predominantly found in deeply eroded craters. A ring syncline (II) and a central uplift (III) are first-order elements following inward. The intensity of faulting and folding increases from I to III. The innermost part of the central uplift often consists of a megabreccia. Both steep to vertical layering and steeply plunging fold axes and fault traces are typical features for the zone surrounding the megabreccia.

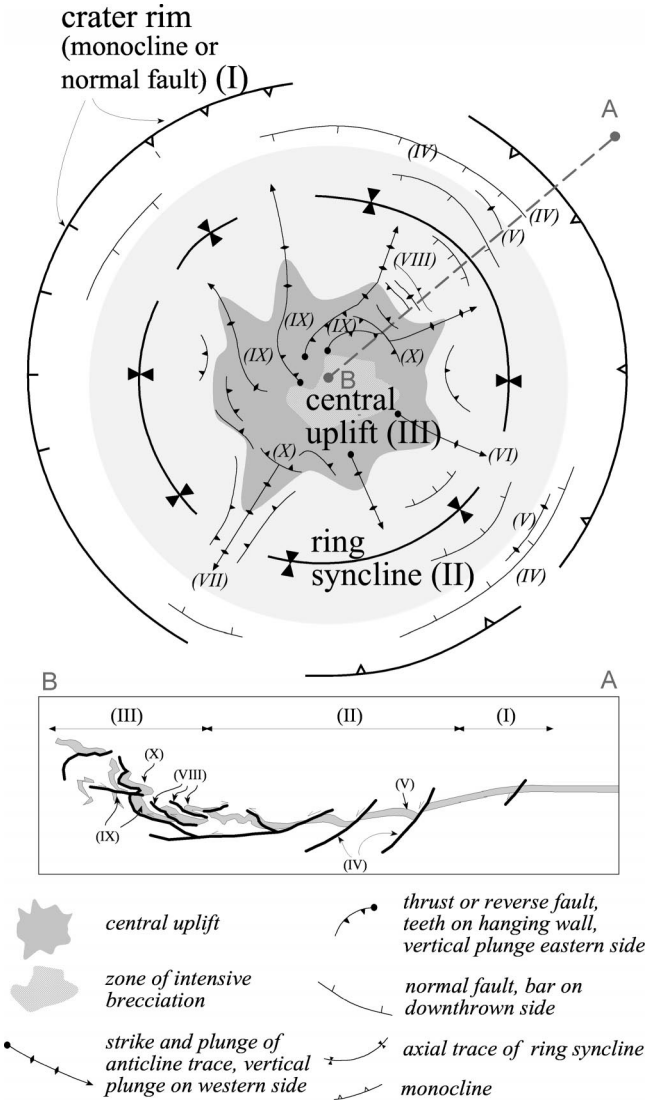

Figure 1. Plan and section views of characteristic deformation pattern in floor of complex terrestrial impact craters of 5–15 km diameter. See text for details.

Second-order elements are listric normal faults of more or less concentric strike (IV), occurring at different positions along the crater rim and within the ring syncline. They usually merge into low-angle detachments at depth (Kenkmann et al., 2000) and compensate for the inward movement of material during crater collapse. In the outer zone, between the crater rim and the ring syncline, detachments dip gently to the crater center. They reverse their inclination on the inner limb of the ring syncline. Detachments are frequently exposed in deeply eroded structures (Kriens et al., 1999). Listric normal faulting is often associated with the formation of rollover antiforms in the hanging wall block (V). The particle trajectory field during inward movement is symmetric with respect to the impact center. Converging particle trajectories can either be compensated by bulk thickening of inward sliding masses, due to folding around concentrically and obliquely striking fold axes, or by the stacking of thrusts sheets (VIII). An alternative accommodation mechanism is the formation of radial anticlines (VI). Radial anticlines plunge outward and increase in volume toward the center of the crater. These radial anticlines are a specific type of so-called radial transpression ridges (VII) (Kenkmann and von Dalwigk, 2000). Within such ridges, material is uplifted or squeezed out to accommodate the converging mass flow. The dip of the hinge line of the radial anticlines increases toward the center of the structure in such a way that vertical or reclined folds develop near the center. It is the radial anticlines and radial transpression ridges that cause the serrated appearance of central uplifts. When a radial anticline is traced along its hinge from the outer parts toward the center of the crater, a gradational transition in fold tightness may be detected, with open symmetrical anticlines changing to isoclinal overturned folds, and fi-

nally merging into fault-propagation folds. Reverse faults start to develop within the core of the folds and extend in area and displacement toward the center. Approaching the inner parts of the central uplift, they eventually form a set of individual thrust sheets, leaning up against the core of the central uplift (IX) (Fig. 1). The mechanism of formation of these thrust lamellae is similar to the closure of an iris of a camera lens, although a bending in the third dimension also occurs. Iris-like thrusts are best exposed in the Spider structure, Australia.

The final structural element typical of complex impact craters consists of recumbent folds, with a concentrically oriented hinge line in the periphery of the central uplift and/or thrusts, where the hanging wall moves outward (X). These features are of subordinate importance in relatively small complex impact structures but become prominent in larger ones, where the central uplift starts to collapse to form a ring. Such deformation elements (X) are capable of compensating for the outward flow during gravity-driven collapse of a central uplift.

STRUCTURAL ANALYSIS OF AN IMPACT-INDUCED FOLD

Despite the complex fold and fault pattern, all these deformation features formed in a similar period of time, which is ~15–60 s for craters of 5–15 km final diameter. To understand the high-strain-rate processes, the microstructure of a representative impact-induced fold of the Crooked Creek impact crater (37°50′N, 91°23′W, ~7 km diameter), Missouri, United States, was investigated in detail. The Crooked Creek impact crater (Hendricks, 1954) is formed in Cambrian to Ordovician sedimentary rocks that are intensely folded, faulted, and brecciated. Outside the crater these rocks are nearly flat-lying. Bounded by a series of normal faults, the structure consists of a peripheral ring syncline that in turns encircles a heavily faulted central uplift. The oldest beds are exposed along a ring anticline of the central uplift and have been uplifted more than 300 m above their normal position (Hendricks, 1954). The innermost part of the central uplift appears to be down-faulted and collapsed. Based on numerical results (Melosh and Ivanov, 1999) and scaling relationships (Melosh, 1989, p. 124), the period of impact crater modification for this crater, which includes the folding event, is ~20–30 s.

Sample Description and Analytical Technique

The analysis concentrated on a single fold (Fig. 2). The sample locality (UTM 4188.750 m N, 641.750 m E) is in the northeast sector of the central uplift at the inner limb of the central uplift ring anticline. The sample is 20 × 15 × 15 cm. Cuttings and thin sections were sawn normal to the fold hinge, which is strongly bent (Fig. 2A). The microstructures were studied using an optical microscope and a scanning electron microscope (JEOL JSM 6300) in backscattered-electron mode.

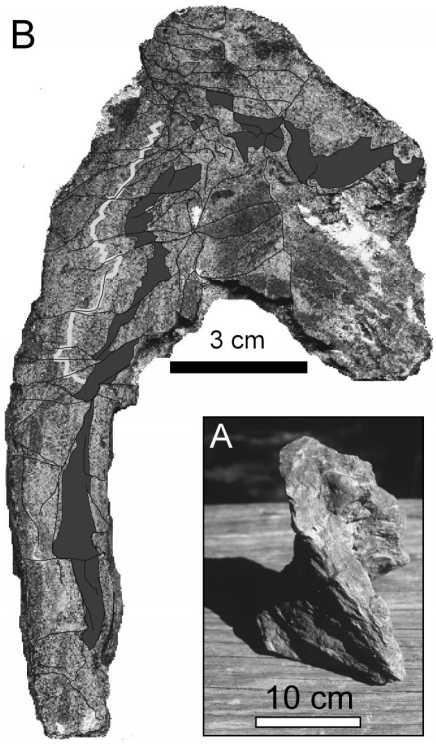

Figure 2. Example of an impact-induced fold within Crooked Creek impact crater. A: Oblique view direction exhibits bended fold hinge. B: Slice of fold normal to hinge line. To emphasize layering and displacements, surface of section was etched with HCl (10%) and then treated with Alizarin S. Shear zones and two marker horizons are retraced for illustration. For description, see text.

RESULTS

Macrostructure

The investigated fold is slightly asymmetric in shape, with a vertical axial surface. The fold hinge strongly bends and plunges steeply to vertically. The interlimb angle of the fold, defined as the angle between the tangents to the two fold limbs constructed at the inflection points (Twiss and Moores, 1992), is 45°–50°. For a geometrical analysis of the fold, the descriptive style elements aspect ratio, tightness, and bluntness are used, which are equant, close, and subangular, respectively. The fold displays a thickened fold hinge and thinned limbs (Fig. 2). This apparent plastic behavior was achieved by localized brittle deformation along millimeter- to centimeter-spaced fault zones and second-order folding. Small-scale shear zones form a network of veins, and their kinematics are inferred from displaced marker horizons. A reduced fault-zone spacing at the fold hinge indicates that microfaults formed syngenetically with the fold. In the fold limbs (Fig. 2), faults form parallel sets of uniform shear sense. Toward the hinge, faults are oriented at an obtuse angle to the layering, become irregularly shaped, and form dense networks. Faulting along planar mechanical anisotropies, such as layer surfaces, is of subordinate importance (Fig. 2). The thickness of some layers changes considerably. Most of the microfaults appear to be shear faults of mode II (sliding parallel to a fracture and perpendicular to the fracture edge).

Microstructure

The investigated fold is built up by stratified impure calcareous dolomites interlayered with layers of calcareous quartz siltstones. Dolomite, quartz, K-feldspar, glauconite, calcite, and hematite are the major constituents of the rock. At the time of impact it was a completely lithified sediment. This is indicated by the fact that the rock matrix (dolomite) and overgrowth seams of the particles are affected by the deformation. Calcite and hematite impregnate the disrupted zones of the rock. The grain sizes of the siliciclastic components are 10–100 μm.

About 40% of grain boundaries are fractured. Grain boundaries between different phases are particularly disrupted. Both open and healed fractures occur, with and without visible displacements. Enhanced fracture densities were observed in process zones around the microshear zones. Toward the shear zones, relict grains become more and more isolated within a fracture network. Deformation is localized into shear zones that typically are 10–500 μm wide (Fig. 3A). The gouge zones of the faults are characterized by reduced grain sizes (down to 1 μm), dominance of angular grain fragments, lack of a preferred alignment of grains, and a multimodal grain-size distribution (Fig. 3B). The gouge-zone thickness, T, increases with increasing fault length and displacement. Displacement, D (in meters), and fault length, L (in meters), scale with $D = 0.56\,L^{1.4}$. Compared with tectonic scaling laws, as reviewed by Scholz (1990) and Clark and Cox (1996), impact-induced faults appear to have anomalously low D/T ratios and anomalously high D/L ratios. A high D/L ratio may indicate a large strain magnitude compensated in the shear zones. Anomalously thick gouge zones are favored by the highly damaged state of the rock, due to dynamic shock fragmentation, prior to shear-zone formation.

Microstructural evidence for plastic deformation, e.g., elongation of grains by superimposed strain, undulose extinction, defor-

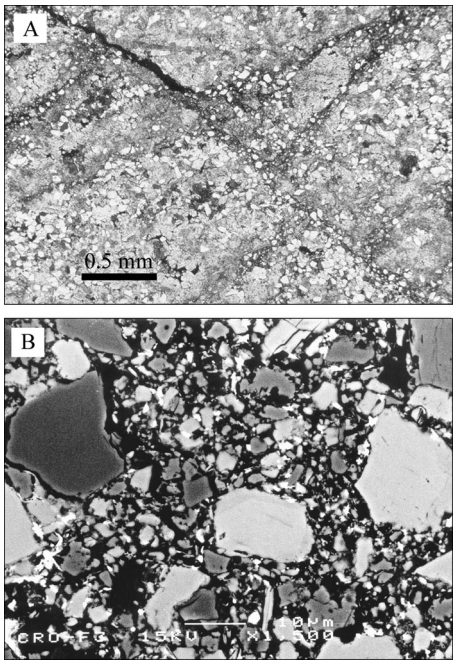

Figure 3. A: Optical micrograph of Crooked Creek fold of Figure 2 displaying several microshear zones, with visible offsets. B: Scanning electron microscope image of microshear zone, with fine-grained quartz (darkest gray), dolomite (dark gray), K-feldspar (light gray), and calcite (lightest gray). Grain-size reduction is due to dynamic fragmentation.

mation twinning, or dynamic recrystallization, was not found in any mineral phase.

DISCUSSION

Folding in impact craters is associated with the gravity-driven collapse of a deep transient cavity and occurs in seconds to minutes. The geometry and orientation of folds change with respect to their position to the crater center (Fig. 1). Folding is generally accommodated by brittle deformation and localized slip on complex shear-zone networks. The collective deformation on the fracture networks causes the apparent ductile behavior of impact-induced folds (limb tightening, fold-axis thickening). The analyzed fold, which serves as a representative for impact-induced folds, yielded no microscopic indications that suggest thermally activated deformation processes induced by postshock heating. Strain rates were too high and temperatures were too low to induce effective plastic flow, within 20–30 s. The dominant feature of the fold consists of the microshear networks (Fig. 3A). Their orientation deviates from common fracture sets associated with folds (e.g., Twiss and Moores, 1992). Faulting along planar mechanical anisotropies, such as layer surfaces, is of subordinate importance. Thus, flexural slip is not a dominant accommodation mechanism of impact folding. Furthermore, the folds are neither shear folds nor volume-loss folds. Similarities to endogenic folds at shallow crustal levels exist (Ismat and Mitra, 2001).

Pervasive shock-induced damage and fracturing, prior to postshock folding and faulting, are of crucial importance for the formation of impact folds. The limit of shock disruption relative to the excavation limit increases with increasing crater size. The intensity of shock damage, i.e., crack density and fragment size, is a function of the distance from the center of the impact (Grady and Kipp, 1987), within the unmodified transient crater cavity. This means that transient cavity collapse that leads to the folding event started in a heavily fractured rock, with a reduced cohesion. The onset of deformation is therefore controlled by the frictional strength of sliding, rather than by the fracture strength of the rock. The fragmented state of the crater floor may also result in an unusually small contact area on impact-induced fault surfaces. This, in turn, may lead to an unusually low friction coefficient and contribute to a soft rheology for the crater floor proposed, e.g., by McKinnon (1978) and Melosh (1979). Structural indications for oscillating movements on fault planes expected for acoustically fluidized rocks (Melosh, 1979) were not unambiguously found in the investigated fold, but can be inferred from other localities.

The analysis of impact-induced folds that are defined in time and space can potentially provide important clues to the formation conditions of tectonic folds; in particular, for those formed at shallow crustal levels. Therefore, this study may stimulate comparative studies between impact-induced and tectonic deformation features.

REFERENCES CITED

Bjørnerud, M.G., 1998, Superimposed deformation in seconds: Breccias from the impact structure at Kentland, Indiana (USA): Tectonophysics, v. 290, p. 259–269.

Clark, R.M., and Cox, S.J.D., 1996, A modern regression approach to determining fault-displacement-length scaling relationships: Journal of Structural Geology, v. 18, p. 147–152.

Grady, D.E., and Kipp, M.E., 1987, Dynamic rock fragmentation, *in* Atkinson, B.K., ed., Fracture mechanics of rock: San Diego, Academic Press, p. 429–475.

Grieve, R.A.F., 1991, Terrestrial impact: The record in the rocks: Meteoritics, v. 26, p. 175–194.

Hendricks, H.E., 1954, The geology of the Steelville Quadrangle, Missouri: Rolla, Missouri Geological Survey and Water Resources, 88 p.

Ismat, Z., and Mitra, G., 2001, Folding by cataclastic flow at shallow crustal levels in the Canyon Range, Sevier orogenic belt, west-central Utah: Journal of Structural Geology, v. 23, p. 355–378.

Kenkmann, T., and von Dalwigk, I., 2000, Radial transpression ridges: A new structural feature of complex impact craters: Meteoritics and Planetary Science, v. 35, p. 1189–1202.

Kenkmann, T., Ivanov, B.A., and Stöffler, D., 2000, Identification of ancient impact structures: Low-angle normal faults and related geological features of crater basements, *in* Gilmour, I., and Koeberl, C., eds., Impacts and the early Earth: Berlin, Springer, p. 271–309.

Kriens, B.J., Shoemaker, E.M., and Herkenhoff, K.E., 1999, Geology of the Upheaval Dome impact structure, southeast Utah: Journal of Geophysical Research, v. 104, p. 18 867–18 887.

Laney, J.E., and Van Schmus, W.R., 1978, A structural study of the Kentland, Indiana, impact site: Lunar Planetary Science Conference Proceedings, v. 9, p. 2609–2639.

McKinnon, W.B., 1978, An investigation into the role of plastic failure in crater modification: Lunar Planetary Science Conference Proceedings, v. 9, p. 3965–3973.

Melosh, H.J., 1979, Acoustic fluidization: A new geologic process?: Journal of Geophysical Research, v. 84, p. 7513–7520.

Melosh, H.J., 1989, Impact cratering: A geological process: New York, Oxford University Press, 245 p.

Melosh, H.J., and Ivanov, B.A., 1999, Impact crater collapse: Annual Review of Earth and Planetary Sciences, v. 27, p. 385–415.

Offield, T.W., and Pohn, H.A., 1979, Geology of the Decaturville impact structure: U.S. Geological Survey Professional Paper 1042, 48 p.

Roddy, D.J., 1979, Structural deformation at the Flynn Creek impact crater, Tennessee: Lunar and Planetary Science Conference Proceedings, v. 10, p. 2519–2534.

Scholz, C., 1990, The mechanics of earthquakes and faulting: Cambridge, UK, Cambridge University Press, 439 p.

Schultz, P.H., and Anderson, R.R., 1996, Asymmetry of the Manson impact structure: Evidence for impact angle and direction: Geological Society of America Special Paper, v. 302, p. 397–417.

Shoemaker, E.M., and Shoemaker, C.S., 1996, The Proterozoic impact record of Australia: AGSO Journal of Australian Geology and Geophysics, v. 16, p. 379–398.

Spray, J.G., 1997, Superfaults: Geology, v. 25, p. 579–582.

Twiss, R.J., and Moores, E.M., 1992, Structural geology: New York, Freeman and Company, 532 p.

Wilshire, H.G., Offield, T.W., Howard, K.A., and Cummings, D., 1972, Geology of the Sierra Madera cryptoexplosion structure, Pecos County, Texas: U.S. Geological Survey Professional Paper 599-H, 42 p.

Manuscript received July 2, 2001
Revised manuscript received October 22, 2001
Manuscript accepted November 26, 2001

Printed in USA